Original Article

Three-dimensional changes of the mandibular arch after total arch distalization in skeletal Class III malocclusion

Youi Sreng[a]; Ji-Hyun Lee[b]; Tung Nguyen[c]; Kee-Joon Lee[d]; Kyung-Ho Kim[e]; Chooryung J. Chung[f]

ABSTRACT

Objectives: To assess three-dimensional (3D) changes in tooth position, arch dimensions, and gingival levels after mandibular total arch distalization in skeletal Class III malocclusion.

Materials and Methods: Skeletal Class III patients treated with mandibular total arch distalization using interradicular temporary anchorage devices were analyzed using stepwise 3D superimposition and reorientation of serial cone beam computed tomography (CBCT) and digital casts ($N = 19$). After mandibular regional superimposition of pre- (T0) and post-treatment (T1) CBCTs, the mandibles were segmented and merged with the corresponding digital casts, generating reoriented, superimposed T0 and T1 digital casts. Changes in individual tooth position, arch dimensions, occlusal plane, and clinical crown height (CCH) were measured.

Results: Mandibular teeth exhibited posterior movement ranging from 1.74 to 2.50 mm with significant lateral movement of the premolars and increase of inter-premolar width by 2.15–2.66 mm ($P < .05$). Extrusive movement of the entire dentition excluding the second molar was noted ($P < .05$), inducing changes of the occlusal plane. The overall changes in CCH were limited to -0.23 to 0.16 mm. CCH significantly increased in the premolars and decreased in the first molar ($P < .05$).

Conclusions: Based on a stepwise digital superimposition, mandibular total arch distalization induced complex 3D changes in the mandibular arch, including distalization, extrusion, and increase of interpremolar width. Gingival margins generally were maintained, though mild-to-moderate recession was suggested in around 20% of the premolars, which may require attention. (*Angle Orthod*. 2025;00:000–000.)

KEY WORDS: Mandibular regional superimposition; Total arch distalization; TADs; CBCT; Digital cast; Gingival recession; Class III

The first two authors contributed equally to this study.

[a] Graduate Student, Department of Orthodontics, Gangnam Severance Hospital, The Institute of Craniofacial Deformity, Yonsei University College of Dentistry, Seoul, Korea.

[b] Professor, Department of Orthodontics, Gangnam Severance Hospital, The Institute of Craniofacial Deformity, Yonsei University College of Dentistry, Seoul, Korea.

[c] Professor, Department of Orthodontics, University of North Carolina School of Dentistry, Chapel Hill, NC, USA.

[d] Professor, Department of Orthodontics, The Institute of Craniofacial Deformity, Yonsei University College of Dentistry, Seoul, Korea.

[e] Professor, Department of Orthodontics, Gangnam Severance Hospital, The Institute of Craniofacial Deformity, Yonsei University College of Dentistry, Seoul, Korea.

[f] Professor and Chair, Department of Orthodontics, Gangnam Severance Hospital, The Institute of Craniofacial Deformity, Yonsei University College of Dentistry, Seoul, Korea.

Corresponding author: Chooryung J. Chung, DDS, PhD, Department of Orthodontics, Gangnam Severance Hospital, The Institute of Craniofacial Deformity, Yonsei University College of Dentistry, #211 Eonjuro, Gangnam-gu, Seoul, Korea
(e-mail: crchung@yuhs.ac)

Accepted: June 19, 2025. Submitted: January 1, 2024.
Published Online: July 28, 2025

INTRODUCTION

The use of temporary anchorage devices (TADs) has broadened the scope of nonsurgical orthodontic treatment by enabling three-dimensional movement of the entire dentition.[1] Total arch distalization with TADs has been reported to address Class II or III malocclusion effectively, while improving vertical and transverse dimensions,[2–5] soft tissue esthetics[6–8] and long-term stability.[9,10] Total arch distalization ranging from 1.29 to 3.5 mm can be successfully achieved using bilateral TADs in the posterior interradicular space of the mandible to improve Class II,[2,11] and Class III malocclusions.[3,12,13]

Clinically, treatment outcome evaluation of total arch distalization has been relatively simplified, mostly by analyzing central incisor and first molar movement using serial lateral cephalometric radiographs.[10,11] Total arch distalization represents movement of the whole arch in the distal direction per se; nevertheless, it induces three-dimensional (3D) changes throughout the entire arch not restricted to the sagittal plane. Cone-beam computed tomography (CBCT) superimposition or best-fit digital model superimposition has suggested various regional extrusive, intrusive, and/or transverse changes affecting arch dimensions,[10,11] and orthopedic changes such as mandibular rotation, possibly inducing changes in the profile as well as smile line.[3,11]

Given the complex dentofacial orthopedic changes induced in the sagittal, vertical, and transverse dimensions after total arch distalization, detailed and accurate 3D evaluation methods are required to fully understand the clinical outcome. However, unlike maxillary CBCT or cast superimposition, which are considered reliable and accurate methods that can be applied clinically,[14–16] mandibular CBCT or cast superimposition is not fully accepted due to various limitations, including lack of stable/reliable anatomical landmarks,[17] late mandibular growth,[18] tooth movement-induced rotation, and the possibility of temporomandibular joint (TMJ) displacement or condylar resorption.[19,20]

Mandibular regional 3D superimposition using volumetric chin and symphysis areas with serial CBCTs has been suggested to address the problem.[21] However, challenges such as separating the arches,[22] and artifacts from metallic restorations or attachments, may hinder tooth identification.[23] Fusing the digital cast to CBCT addresses this issue, providing reliable, detailed tooth and arch surfaces.[24,25] Stepwise mandibular regional superimposition with digital cast fusion offers reliable reorientation and precise morphology of the dentition, including gingival margins, without interferences of the maxillary dentition, and mandibular positional or growth changes.

Therefore, the current study aimed to assess 3D mandibular tooth displacement, changes in arch dimensions and gingival margins after mandibular total arch distalization with interradicular TADs in Class III malocclusion by using a stepwise 3D mandibular CBCT superimposition followed by digital cast superimposition.

MATERIALS AND METHODS

Subjects

This study was approved by the institutional review board of Gangnam Severance Hospital (IRB No. 3-2023-0479).

Consecutive patients: (1) diagnosed with skeletal Class III malocclusion (ANB < 0) with full dentition excluding third molars; (2) who underwent mandibular total arch distalization with interradicular TADs along with fixed appliances; and (3) with full records, including pretreatment (T0) and post-treatment (T1) CBCTs, treated at the Department of Orthodontics, Gangnam Severance Hospital, were collected retrospectively. Patients with: (1) extraction of teeth other than third molars, (2) who underwent orthognathic surgery, (3) with severe asymmetry (menton deviation > 4 mm), and (4) poor CBCT or digital cast image quality were excluded.

Based on a previous report on total distalization using TADs,[11] the sample size was estimated as 16 to identify an effect size of 1.17 ($\alpha = 0.05$, $\beta = 0.01$). Considering dropouts, 19 subjects (22.53 ± 7.8 years) were included for the study (Table 1). After levelling and alignment using Roth prescription self-ligating brackets, buccal interradicular TADs were inserted between the mandibular second premolar and first molar, or the first and second molars, bilaterally. Elastomeric chains were applied from the TADs to the crimpable long-hooks on the anterior segment for distalization. Cephalometric changes at T0 and T1 indicated mandibular total arch distalization (Table 2).

CBCT scans (Pax-zenith 3D; Vatech, Seoul, South Korea) were obtained at 120 kV and 10 mA, voxel size 0.3 nm, and rotation time 24 s. The patients were scanned in a natural head posture in maximum intercuspal position. T0 scans were taken for orthodontic diagnostic purposes. Given that the subjects underwent skeletal Class III camouflage treatment, T1 scans were taken for reasons including the evaluation of detailed 3D orthodontic treatment outcomes, periodontal conditions, assessment of airway, as well as TMJ position. Digital casts were produced using a digital model scanner (DOF Freedom HD; DOF, Seoul, Korea) or directly scanned using an intraoral iTero 5D Element scanner (Align Technology, Santa Clara, USA).

Table 1. Subject Characteristics

Host Characteristics	N
Age (13–45 y)	
10 s	9
20 s	8
30 s	1
40 s	1
Skeletal maturity index (SMI)	
SMI 10	3
SMI 11	16
Sex	
F	10
M	9
Arch Length Discrepancy	
Mild (0–3 mm)	13
Moderate (4–6 mm)	3
Spacing (<0 mm)	3
Anterior crossbite	
Yes	4
Edge to edge	6
No	9
Posterior crossbite	
Yes	6
No	13
Vertical Facial Pattern	
Hypodivergent (FMA < 21°)	5
Normodivergent (21° ≤ FMA ≤ 29°)	12
Hyperdivergent (FMA > 29°)	2

Table 2. Cephalometric Analysis[a,b]

	Pretreatment (T0)		Posttreatment (T1)		
Parameters	Mean	SD	Mean	SD	*P* Value
SNA (°)	81.82	3.58	82.25	3.20	.13
SNB (°)	82.98	3.68	82.66	3.47	.20
ANB (°)	−1.16	0.82	−0.40	1.48	.01*
Wits Appraisal (mm)	−6.66	3.19	−4.80	2.41	<.001**
FMA (°)	23.60	4.91	23.69	4.64	.72
SN -U1 (°)	113.07	8.09	112.61	7.27	.57
L1-Mp (°)	89.66	6.20	85.05	6.44	<.001**
Incisal Angle (°)	125.11	8.84	130.26	7.56	<.001**
SN-MP (°)	32.22	5.87	32.00	5.88	.40
SN-OP (°)	14.08	5.87	13.00	5.48	.02*
Overbite	0.42	1.24	1.64	1.05	<.001**
Overjet	1.36	2.11	4.00	1.48	<.001**

[a] Paired *t*-test between T0 and T1, * $P < .05$; ** $P < .001$.
[b] SD, standard deviation.

Stepwise Registration and Superimposition of the Mandible

Step 1. Registration and reorientation: Mandibular regional superimposition. T0 and T1 CBCTs were superimposed using a voxel based regional mandibular superimposition method with ITK snap (Version 4.0.2; http://www.itksnap.org).[21] Stable anatomical references including the inner cortical surface of the inferior border of the symphysis and the anterior surface of the chin above pogonion were set. 3D masks of the chin (Figure 1A, red) and symphysis (Figure 1a, blue) were created from the T0 CBCT. The T1 CBCT was then imported and superimposed onto T0 using the previously created 3D surface masks, reorienting the T1 to the T0 CBCT (Figure 1a, box).

Step 2. Mandibular segmentation: 3D mandibular Models. T0 and reoriented T1 CBCT volumes were segmented to generate 3D mandibular models (Figure 1B, green and red) using 3D Slicer 5.4.0 (http://www.slicer.org).

Step 3. Fusion of 3D mandibular models and digital casts. The segmented mandibular models and the corresponding digital casts were fused using Slicer Craniomaxillofacial (CMF) registration, based on the Iterative Closest Point algorithm.[26] Regions of interest (ROIs) were defined by positioning four points: the cusp tips of both canines and central fossae of either the first or the second molars (Figure 1C, red), aligning the digital casts to the 3D mandibular models.[26]

Step 4. Mandibular cast superimposition and landmark positioning. T0 and T1 mandibular casts were superimposed and registered, sharing the same orientation. A representative landmark was placed on each tooth: L1 and L2, midpoints of the incisal edge; L3, canine cusp tip; L4 and L5, buccal cusp tip or highest point of the premolars; and L6 and L7, mesiobuccal cusp tip or highest point of the molars (Figure 1D).

3D Displacement of the Mandibular Teeth and Changes in Arch Dimensions

Tooth displacement was assessed using the coordinates of two designated landmarks on the T1 and T0 models (Δx, Δy, Δz). Δx, Δy, and Δz represented the transverse (+lateral; - median), sagittal (+mesialized; −distalized), and vertical (+extrusive; −intrusive) changes, respectively. Intercanine, premolar, molar widths were calculated as the direct distance between the left and right landmarks. Changes in arch width (T1–T0) were classified as decreased (<−1 mm), maintained (−1 mm to + 1 mm), or increased (>1 mm).

Changes in the Occlusal Plane

The occlusal plane was defined as a plane passing through the left and right mesial buccal cusp tips of the lower first molars and the midpoint of the lower central incisor landmarks. Changes were measured as the angle between the T0 (Figure 2, green line) and T1

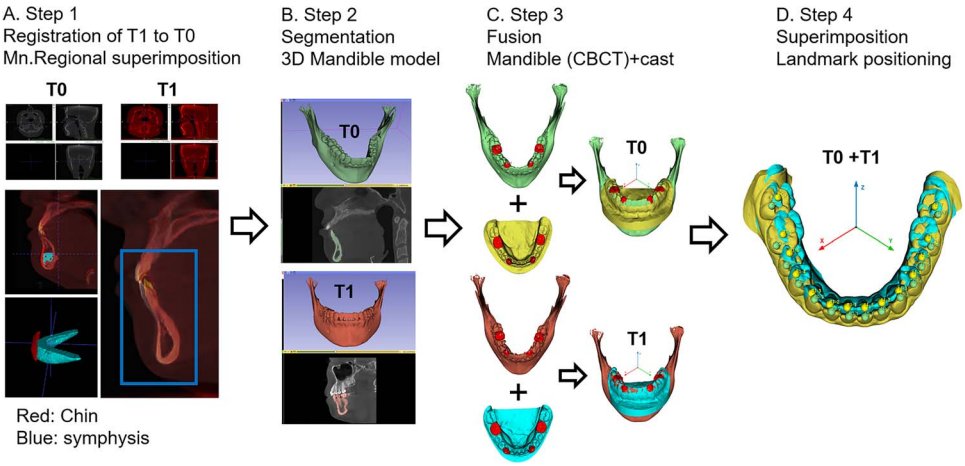

Figure 1. Schematic illustration of the stepwise 3D registration and superimposition of serial CBCTs and digital casts. CBCT, cone beam computed tomography. (A) Mandibular regional superimposition. Anterior surface of the chin above pogonion (red) and the inner cortical surface of the inferior border of the symphysis (blue) were used as references. (B) Segmentation of the mandible to generate the 3D mandibular models. (C) Fusion of the corresponding digital casts to CBCTs using both the canine and first molar surfaces (red). (D) Superimposed and reoriented digital mandibular casts on T0 CBCT images.

(Figure 2, red line) planes, and classified as clockwise rotation, counterclockwise rotation, intrusion and extrusion, or left and right rotation (Figure 2).

Changes in Clinical Crown Height and Gingival Recession

Changes in the marginal gingiva were indirectly assessed via changes in clinical crown height (ΔCCH).[27,28] CCH was measured as the distance from the mid-developmental ridge or the mesiobuccal cusp tip to the buccal surface of the crown and gingival contact point along the crown axis. ΔCCH was calculated as the absolute difference between T1 and T0 CCH, with + indicating gingival gain and – indicating recession. ΔCCH was subclassified into gingival gain (>0.5 mm), maintained (−0.5 mm to + 0.5 mm), mild recession (>−2 to < −0.5 mm), and moderate recession (≤−2 mm).[28]

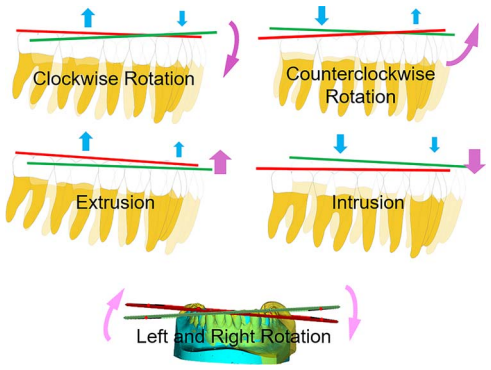

Figure 2. *Schematic illustration of occlusal plane changes* after *total arch distalization.* The occlusal plane (T0 in green and T1 in red) was defined as the plane passing through the mesial buccal cusp tips of the first molars and the midpoint of the lower central incisor landmarks. Blue arrow: direction of tooth movement; purple arrow: change in the occlusal plane.

Statistical Analysis

Sample size was calculated with G*Power (Heinrich Heine Universität, Düsseldorf, Germany). Measurement reliability was performed by two examiners (YI, SD) independently, with 10 randomly selected samples reassessed at a 2-week interval. Intra-examiner correlation coefficients ranged from r = 0.90–0.99 and interexaminer correlation coefficients ranged from 0.70 to 0.98. Shapiro–Wilk tests confirmed the normal distribution of variables. Paired *t*-tests (IBM SPSS Statistics v. 21.0, Chicago, USA) were used to compare T0 and T1 measurements, with a significance level set at $P < .05$.

RESULTS

3D Changes in the Mandibular Arch After Total Arch Distalization

The most prominent changes occurred in the sagittal plane (Δy), with significant distalization of 1.74–2.50 mm ($P < .001$). The first and second premolars and second molars showed significant lateral transverse (Δx) movement ($P < .05$). All teeth except the second molars exhibited significant extrusive vertical (Δz) movement ($P < .001$) (Table 3).

Changes in Arch Width After Total Arch Distalization

Interpremolar widths increased significantly ($P < .05$) (Table 4). Subclassification revealed inter-first

Table 3. 3D Displacement of the Mandibular Teeth After Total Arch Distalization[a–c]

Mandibular Tooth (N = 38)	Transverse (Δx, mm)			Sagittal (Δy, mm)			Vertical (Δz, mm)		
	Mean	SD	*P* Value	Mean	SD	*P* Value	Mean	SD	P Value
Central Incisor	0.05	0.87	.72	−2.12	1.93	<.001**	0.94	1.19	<.001**
Lateral Incisor	0.18	1.25	.38	−1.74	2.20	<.001**	0.55	0.98	<.001**
Canine	−0.06	1.45	.79	−2.14	1.49	<.001**	0.52	0.86	<.001**
First Premolar	0.72	1.59	.01*	−1.83	1.58	<.001**	0.94	0.80	<.001**
Second Premolar	0.84	1.53	<.001**	−1.91	1.86	<.001**	1.11	0.84	<.001**
First molar	0.03	1.15	.79	−2.17	1.46	<.001**	0.81	0.82	<.001**
Second Molar	0.44	1.29	.04*	−2.50	1.66	<.001**	0.02	0.98	.87

[a] Transverse Δx (+: lateral, −: medial); Sagittal Δy (+: mesialized, −: distalized); Vertical Δz (+: extrusive, -: intrusive)
[b] Paired *t*-test between T0 and T1, * $P < .05$; ** $P < .001$.
[c] SD indicates standard deviation.

and second premolar widths increased by 52.6 (10/19) to 57.9% (11/19) of the subjects, exceeding the 5.3 (1/19) to 15.8% (3/19) of subjects with decreased width. Intercanine, first and second molar widths were primarily maintained in 68.4% (13/19) and 42.1% (8/19), of subjects, respectively.

Change in the Occlusal Plane After Total Arch Distalization

Extrusion of the occlusal plane was most frequently noted, in 42.1% of the subjects (8/19), followed by clockwise rotation in 21.1% (4/19) (Table 5).

Changes In CCH and Gingival Recession After Total Arch Distalization

ΔCCH were limited to −.23 to 0.16 mm. CCH significantly increased in the first and second premolars, suggesting gingival recession, while it significantly decreased in the first molar, indicating gingival gain ($P < .05$) (Table 6).

Overall, CCH was maintained in 72.5% (193/266) of the teeth evaluated. Mild to moderate recession was most prominently detected in the first (8/38) and second premolars (9/38). Gingival gain was noted in the central incisors (9/38) and the first (9/38) and second molars (8/28).

DISCUSSION

Stepwise superimposition revealed detailed treatment outcomes of mandibular total arch distalization in skeletal Class III malocclusion. Along with distal movement of the whole dentition, extrusion, occlusal plane changes, and increase in interpremolar widths highlighted complex 3D changes following treatment. Gingival margins were generally maintained, though mild-to-moderate recession was observed in around 20% of the premolars.

Voxel-based regional mandibular superimposition using serial CBCTs differentiated changes in the mandibular dentition by eliminating confounding factors affecting mandibular position, such as maxillary dental interferences, mandibular growth dynamics, rotational effects induced by tooth movement, and the potential occurrence of temporomandibular joint (TMJ) displacement or condylar resorption.[18–20] The stepwise registration of digital casts also compensated for the absence of reliable intraoral landmarks, enabling precise visualization of tooth surfaces and gingival margins.[17,24,25]

Based on the results, the second molar showed the largest amount of distalization, while vertical and lateral displacements were most prominent in first and second premolars. Excessive buccal expansion or tipping may lead to gingival recession[29,30] and extrusion may increase CCH.[31] The combined movement of the

Table 4. Changes in Arch Width After Mandibular Total Arch Distalization[a,b]

Arch Width	T0 (mm)		T1 (mm)		T1–T0 (mm)		
	Mean	SD	Mean	SD	Mean	SD	*P* Value
Intercanine	27.69	1.81	27.54	1.22	−0.14	1.99	.76
Interfirst premolar	35.68	2.45	37.13	1.44	1.45	2.66	.03*
Intersecond premolar	41.76	2.60	43.42	1.70	1.66	2.15	<.001**
Interfirst molar	47.73	2.61	47.78	2.42	0.05	1.77	.90
Intersecond molar	53.80	3.46	54.67	2.71	0.87	1.97	.07

[a] Paired *t*-test between T0 and T1, * $P < .05$; ** $P < .001$.
[b] SD indicates standard deviation.

Table 5. Changes in the Occlusal Plane After Mandibular Total Arch Distalization[a]

Changes in Occlusal Plane	N, Incidence (%)	Degree of Change Mean ± SD (°)
Clockwise rotation	4 (21.1)	−3.62 ± 1.16
Counterclockwise rotation	3 (15.8)	2.51 ± 1.6
Extrusion	8 (42.1)	−1.08 ± 1.07
Intrusion	2 (10.5)	1.42 ± 0.87
Left-right rotation	2 (10.5)	0.69 ± 0.44
Total	19 (100)	

[a] SD indicates standard deviation.

first and second premolars likely contributed to the increase in CCH and greater incidence of gingival recession compared to other teeth.[27] Overall, the average CCH changes were limited to 0.23 mm, consistent with a previous study.[27] Nevertheless, the results should be interpreted cautiously, as patients were relatively young and healthy with no history of periodontal issues. Gingival recession is multifactorial and influenced by host factors such as age, biotype, and oral hygiene, in addition to treatment effects.[32] Thus, high-risk groups and long-term prognosis should be carefully monitored. Interestingly, CCH decreased in the first molars, and gingival gain was noted to some degree among the central incisors and the molars. This indicated the versatile response of the periodontal soft tissue after orthodontic tooth movement. The improvement of incisal position as well as buccal overjet may have resulted in the morphologic gain of the gingival level relative to the tooth crown.

Arch width increases were similar to previous reports,[10,11] with significant lateral displacement noted in the premolars and the second molar. Biomechanically, buccal tipping is well-accepted and expected when using buccal mechanics with buccal interradicular TADs.[11,33] The lack of buccal displacement of the first molar may reflect a focus on skeletal Class III treatment, often involving initial buccal crossbites and the continuous management of arch coordination to not increase buccal overjet specifically.[34,35] However, given that the results were based on the displacement pattern of crown landmarks, the increase or decrease of arch width may not represent pure changes at the root level. Further evaluation of the root displacement pattern would provide a more comprehensive understanding of the arch dimensions.

Vertically, occlusal plane changes were mainly observed as overall extrusion of the incisors and molars or clockwise rotation. These results were rather contradictory to previous findings indicating molar intrusion resulting in 1.3°–3.2° counterclockwise rotation after mandibular distalization.[3,12,36] This variation may be attributed to differences in 2-dimensional (2D) cephalometric, vs 3D imaging, methods, and evaluation techniques. Notably, this study was designed to eliminate the interference of mandibular rotation that may influence the interpretation of pure changes in the vertical dimension.

Due to its retrospective design and difficulties in acquiring interim CBCTs, assessments were based on pre-existing before-and-after records that represent the overall outcome of comprehensive orthodontic treatment encompassing all stages of tooth movement not solely limited to mandibular total arch distalization. For example, initial leveling of the Curve of Spee may have resulted in extrusion of the premolars while uprighting posterior teeth that were inclined lingually, may have affected interpremolar width, consequently changing the CCH and gingival margins. To overcome some of the limitations, efforts were made to ensure homogeneity by selecting skeletal Class III adults with a primary treatment objective focused on mandibular total arch distalization after a standardized protocol using interradicular TADs in the mandibular molar region.

Clinically, total arch distalization may inadvertently induce mandibular arch expansion, resulting in buccal crossbite given that patient with skeletal class III malocclusion are prone to have preexisting transverse discrepancies. Thorough pretreatment evaluation focusing on transverse dimensions as well as incorporating

Table 6. Changes in Clinical Crown Height After Mandibular Total Arch Distalization[a,b]

Clinical Crown Height (CCH)	T0 (mm)		T1 (mm)		T1–T0 (mm)		
	Mean	SD	Mean	SD	Mean	SD	*P* Value
Central Incisor	8.31	0.76	8.22	0.93	0.08	0.49	.29
Lateral Incisor	8.47	0.74	8.43	0.87	0.02	0.42	.59
Canine	10.10	1.01	10.05	0.91	−0.05	0.35	.41
First Premolar	8.56	0.81	8.71	0.87	−0.15	0.40	.02*
Second Premolar	7.34	0.72	7.57	0.76	−0.23	0.58	.02*
First molar	6.94	0.62	6.78	0.82	0.16	0.44	.03*
Second Molar	6.31	0.80	6.19	0.74	0.12	0.71	.32

[a] Paired *t*-test between T0 and T1, * $P < .05$.
[b] SD indicates standard deviation.

biomechanical compensatory strategies, such as optimization of force vectors, application of maxillary expansion or cross elastics and modifications in the archwire with toe-in bends or lingual torque, etc., can be strategically applied to mitigate the adverse effects. Because changes in the vertical dimension and occlusal plane can cause changes in the soft tissue profile, close monitoring of the overall dentofacial changes is also recommended.

Despite the retrospective nature of the study, stepwise registration using 3D digital imaging has contributed to the understanding of 3D individual tooth movement after total arch distalization in skeletal Class III malocclusion.

CONCLUSIONS

- Stepwise digital superimposition enabled visualization of 3D treatment outcomes after mandibular total arch distalization using interradicular TADs in skeletal Class III malocclusion.
- Together with distalization, extrusion and an increase of interpremolar width were noted.
- Although changes in the gingival margins were limited, a few instances of mild-to-moderate recession were noted in the first and second premolars.

ACKNOWLEDGMENTS

This research was supported by Yonsei University College of Dentistry (6-2020-0026). The authors declare no potential conflicts of interest regarding the authorship and/or publication of this article.

REFERENCES

1. Proffit WR, Fields H, Larson B, Sarver DM. *Contemporary Orthodontics*. St Louis: Mosby; 2018.
2. Bechtold TE, Kim JW, Choi TH, Park YC, Lee KJ. Distalization pattern of the maxillary arch depending on the number of orthodontic miniscrews. *Angle Orthod*. 2013;83:266–273.
3. Nakamura M, Kawanabe N, Kataoka T, Murakami T, Yamashiro T, Kamioka H. Comparative evaluation of treatment outcomes between temporary anchorage devices and Class III elastics in Class III malocclusions. *Am J Orthod Dentofacial Orthop*. 2017;151:1116–1124.
4. Lee KJ, Kim SJ. Advanced biomechanics for total arch movement and non-surgical treatment for hyperdivergent faces. *Semin Orthod*. 2018;24:83–94.
5. Nguyen T, Baek ES, Hwang S, Kim KH, Chung CJ. Nonsurgical and nonprosthetic camouflage treatment of skeletal Class II open bite with bilaterally missing lower first molars. *Angle Orthod*. 2019;89:505–517.
6. Baek ES, Hwang S, Kim KH, Chung CJ. Total intrusion and distalization of the maxillary arch to improve smile esthetics. *Korean J Orthod*. 2017;47:59–73.
7. Baek ES, Hwang S, Choi YJ, et al. Quantitative and perceived visual changes of the nasolabial fold following orthodontic retraction of lip protrusion. *Angle Orthod*. 2018; 88:465–473.
8. Park YS, Choi JH, Kim Y, et al. Deep learning-based prediction of the 3D postorthodontic facial changes. *J Dent Res*. 2022;101:1372–1379.
9. Bechtold TE, Park YC, Kim KH, Jung H, Kang JY, Choi YJ. Long-term stability of miniscrew anchored maxillary molar distalization in Class II treatment. *Angle Orthod*. 2020;90: 362–368.
10. Song BJ, Lee KJ, Cha JY, Lee JS, Mo SS, Yu HS. Stability of the maxillary and mandibular total arch distalization using temporary anchorage devices (TADs) in adults. *Appl Sci-Basel*. 2022;12.
11. Oh YH, Park HS, Kwon TG. Treatment effects of microimplant-aided sliding mechanics on distal retraction of posterior teeth. *Am J Orthod Dentofacial Orthop*. 2011;139: 470–481.
12. Yeon BM, Lee NK, Park JH, Kim JM, Kim SH, Kook YA. Comparison of treatment effects after total mandibular arch distalization with miniscrews vs ramal plates in patients with Class III malocclusion. *Am J Orthod Dentofacial Orthop*. 2022;161:529–536.
13. Sugawara J, Daimaruya T, Umemori M, et al. Distal movement of mandibular molars in adult patients with the skeletal anchorage system. *Am J Orthod Dentofacial Orthop*. 2004; 125:130–138.
14. Vasilakos G, Schilling R, Halazonetis D, Gkantidis N. Assessment of different techniques for 3D superimposition of serial digital maxillary dental casts on palatal structures. *Sci Rep*. 2017;7:5838.
15. Jang W, Choi YJ, Hwang S, Chung CJ, Kim KH. Anchorage loss assessment of the indirect anchor tooth during adjunctive orthodontic treatment. *Am J Orthod Dentofacial Orthop*. 2019;155:347–354.
16. Chung CJ, Jang W, Piers C, et al. Differential alveolar bone modeling after orthodontic retraction. *J Am Dent Assoc*. 2019;150:313–320.
17. Stucki S, Gkantidis N. Assessment of techniques used for superimposition of maxillary and mandibular 3D surface models to evaluate tooth movement: a systematic review. *Eur J Orthod*. 2020;42:559–570.
18. Ruellas AC, Yatabe MS, Souki BQ, et al. 3D mandibular superimposition: comparison of regions of reference for voxel-based registration. *PLoS One*. 2016;11:e0157625.
19. Koerich L, Weissheimer A, de Menezes LM, Lindauer SJ. Rapid 3D mandibular superimposition for growing patients. *Angle Orthod*. 2017;87:473–479.
20. Park TJ, Lee SH, Lee KS. A method for mandibular dental arch superimposition using 3D cone beam CT and orthodontic 3D digital model. *Korean J Orthod*. 2012;42: 169–181.
21. Nguyen T, Cevidanes L, Franchi L, Ruellas A, Jackson T. Three-dimensional mandibular regional superimposition in growing patients. *Am J Orthod Dentofacial Orthop*. 2018; 153:747–754.
22. Chen Y, Du H, Yun Z, et al. Automatic segmentation of individual tooth in dental CBCT images from tooth surface map by a multi-task FCN. *IEEE Access*. 2020;8:97296–97309.
23. Swennen GR, Barth EL, Eulzer C, Schutyser F. The use of a new 3D splint and double CT scan procedure to obtain an accurate anatomic virtual augmented model of the skull. *Int J Oral Maxillofac Surg*. 2007;36:146–152.

24. Park JH, Hwang CJ, Choi YJ, et al. Registration of digital dental models and cone-beam computed tomography images using 3-dimensional planning software: comparison of the accuracy according to scanning methods and software. *Am J Orthod Dentofacial Orthop*. 2020;157:843–851.
25. Uechi J, Tsuji Y, Konno M, et al. Generation of virtual models for planning orthognathic surgery using a modified multimodal image fusion technique. *Int J Oral Maxillofac Surg*. 2015;44:462–469.
26. Garib D, Miranda F, Yatabe MS, et al. Superimposition of maxillary digital models using the palatal rugae: does ageing affect the reliability? *Orthod Craniofac Res* 2019;22: 183–193.
27. Tsukada K, Ozeki Y, Sato C, Fushima K. Clinical crown height changes in adult patients after non-extraction, orthodontic treatment: a retrospective cohort study. *J Orthod*. 2023:14653125231217756.
28. Handelman CS, Eltink AP, BeGole E. Quantitative measures of gingival recession and the influence of gender, race, and attrition. *Prog Orthod.* 2018;19:5.
29. Andlin-Sobocki A, Bodin L. Dimensional alterations of the gingiva related to changes of facial/lingual tooth position in permanent anterior teeth of children. A 2-year longitudinal study. *J Clin Periodontol*. 1993;20:219–224.
30. Kraus CD, Campbell PM, Spears R, Taylor RW, Buschang PH. Bony adaptation after expansion with light-to-moderate continuous forces. *Am J Orthod Dentofacial Orthop*. 2014; 145:655–666.
31. Kajiyama K, Murakami T, Yokota S. Gingival reactions after experimentally induced extrusion of the upper incisors in monkeys. *Am J Orthod Dentofacial Orthop*. 1993;104: 36–47.
32. Kassab MM, Cohen RE. The etiology and prevalence of gingival recession. *J Am Dent Assoc*. 2003;134:220–225.
33. Oh MB, Mo SS, Hwang CJ, Chung C, Kang JM, Lee KJ. The 3-dimensional zone of the center of resistance of the mandibular posterior teeth segment. *Am J Orthod Dentofacial Orthop*. 2019;156:365–374.
34. Ahn J, Kim SJ, Lee JY, Chung CJ, Kim KH. Transverse dental compensation in relation to sagittal and transverse skeletal discrepancies in skeletal Class III patients. *Am J Orthod Dentofacial Orthop*. 2017;151:148–156.
35. Kim HJ, Jang WS, Park HS. Anatomical limits for distalization of lower posterior molars with micro-implant anchorage. *J Clin Orthod*. 2019;53:305–313.
36. Kook YA, Choi TH, Park JH, Kim SH, Lee NK. Comparison of posttreatment stability after total mandibular arch distalization with mini-implants and mandibular setback surgery. *Angle Orthod*. 2024;94:159–167.